Journal of the Korean Crystal Growth and Crystal Technology
Vol. 35, No. 2 (2025) 71-78
https://doi.org/10.6111/JKCGCT.2025.35.2.071

p-ISSN 1225-1429
e-ISSN 2234-5078

Study on the feasibility of metallic saggar for synthesizing NCM cathode active materials-II

Sung Hyun Woo*,**, Jihun Jung*,**, Sehyun Oh*,**, Jung Heon Lee** and Hyeong-Jun Kim*,†

**Engineering Material Center, Korea Institute of Ceramic Engineering & Technology, Icheon 17303, Korea*
***Department of Advanced Materials Science & Engineering, Sungkyunkwan University, Suwon 16419, Korea*

(Received May 21, 2025)
(Revised May 29, 2025)
(Accepted June 13, 2025)

Abstract Nickel has excellent oxidation resistance and high thermal stability, making it a promising candidate for use as a saggar material. Additionally, as it has a composition similar to that of nickel–cobalt–manganese (NCM), it exhibits low reactivity with cathode active materials. Thus, this study proposes metallic nickel as a saggar material for the synthesis of NCM [$Li(Ni_xCo_yMn_z)O_2$] cathode active materials. A long-term reaction test was conducted at 900°C between a nickel crucible and an $LiNi_{0.8}Co_{0.1}Mn_{0.1}O_2$ precursor to evaluate the effectiveness of the proposed strategy. The results show that an (NiO_x) reaction layer was formed on the surface of the nickel crucible due to oxygen diffusion from the cathode precursor oxide and its reaction with atmospheric oxygen. This NiO layer also contributed to an increase in surface hardness. As the heat-treatment time increased, the thickness of the reaction layer gradually increased, exceeding 156 μm, and after 480 h, the erosion depth of the crucible was 2~3 times greater when the precursor contained Li compared to when it did not. Nevertheless, the nickel crucible maintained its shape even after continuous reaction with Li-containing NCM precursors for more than 20 d, confirming its suitability for use as a saggar in NCM synthesis.

Key words Cathode material, NCM, Nickel, Nickel oxide, Saggar, Synthesis

1. Introduction

Lithium-ion batteries (LIBs) have been established as the primary power source for eco-friendly vehicles due to their high energy density and efficient energy storage and discharge performance [1,2]. Over the past decade, the market share of LIBs in the hybrid and electric vehicle (EV) sector has steadily increased, with reports indicating an expansion of over 20 %. In particular, market demand is rapidly increasing as lithium-ion secondary batteries, which provide high energy density and high voltage, have become practical for large-scale applications [3-6]. Accordingly, many countries are actively developing next-generation secondary batteries that offer high stability and improved energy storage capacity.

Nickel-cobalt-manganese (NCM) materials, one of the cathode active materials in LIBs, are composed of metal oxide complexes, including lithium, nickel, cobalt, and manganese. These materials have evolved from the layered structure of $LiCoO_2$, which was developed in the 1980s. Recent research focuses on increasing the nickel content to enhance the specific capacitance of NCM materials, while reducing the cobalt content to lower costs and improve sustainability. Accordingly, the nickel-rich composition of $LiNi_{0.8}Mn_{0.1}Co_{0.1}O_2$ (NCM811) is gaining significant attention and is being researched as a key material for high-capacity and high-power batteries [6,7].

The saggar used in the manufacturing of NCM materials is generally composed of cordierite ($2MgO \cdot 2Al_2O_3 \cdot 5SiO_2$), which has a low thermal expansion coefficient, high thermal shock resistance, and creep resistance. However, during the firing process, the formation of Li_2O induces cracks in the saggar, significantly reducing its lifespan, particularly in high-temperature environments above 900°C [8]. Additionally, ceramic-based saggars are typically used fewer than 20 times, and in many cases, they are used even less frequently. Furthermore, reactions with cathode active materials lead to the incorporation of impurities, which considerably degrade product quality [9-14]. In particular, environmental pollution both inside and outside manufacturing plants due to discarded saggars has become a significant concern.

Nickel has a high melting point (1,453°C) and excellent oxidation resistance [15]. Therefore, a Ni crucible is expected to minimize quality degradation caused by contamination, as its composition is identical to that of

---

[†] Corresponding author
E-mail: goldbud@kicet.re.kr

Ni, the primary component of NCM-based cathode active materials. In a previous study, $Ni_{0.80}Co_{0.10}Mn_{0.10}(OH)_2$, which exclude Li, was used to analyze erosion depth and diffusion rate, and preliminary tests were conducted to assess the feasibility of using Ni crucibles as saggars [16].

The present study evaluates the reaction stability between the NCM 811 precursor and the Ni crucible. By comparing and analyzing the diffusion reaction rate and growth behavior of NiOx at the interface between Li-containing NCM and the Ni crucible with findings from previous studies, the lifespan of the Ni crucible was predicted, and its applicability as a saggar was examined.

2. Experimental

2.1. Materials

The starting materials used were $Ni_{0.8}Co_{0.1}Mn_{0.1}$ $(OH)_2$ and $LiOH·H_2O$ (≥98.0 %, Sigma-Aldrich). To compensate for lithium loss during the synthesis process, $Ni_{0.8}Co_{0.1}Mn_{0.1}(OH)_2$ and $LiOH·H_2O$ were mixed in a molecular ratio of 1:1.05. NCM 811 was mixed for 10 min using a resonance mixer (Lab RAM, RESODYN, USA).

A nickel metallic crucible (≥99.0 wt.% purity) with an outer diameter of 37 mm, a height of 39 mm, a thickness of 0.78 mm, and a capacity of 30 mL was prepared. One of these saggars was not heat-treated and was used as the control.

As the precursor for the erosion reactivity analysis of the bottom surface of the Ni metallic crucible, 6 mL of NCM811 was introduced into the crucible. Subsequently, the Ni metallic crucibles containing the cathode precursor oxide were subjected to heat treatment in a furnace under atmospheric pressure, with each crucible subjected to different heat-treatment conditions, as specified in Table 1.

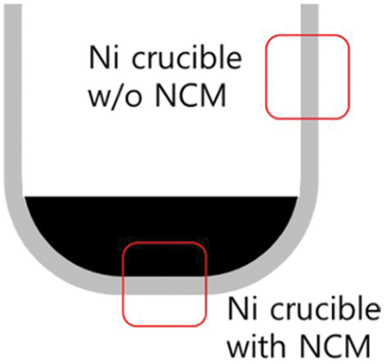

Fig. 1. Schematic of the nickel crucible used in the study [16].

Table 1
Heat-treatment temperature and time conditions for Ni crucibles

Specimen number	Time (h)	Temperature (°C)
#a	12	900
#b	24	
#c	72	
#d	480	

2.2. Microstructure analysis

Field emission scanning electron microscopy (FE-SEM, JSM-7500F, JEOL, Japan) was used to identify the compounds formed by the diffusion reaction at the interface and to measure the thickness of the reaction layer. To analyze the composition and distribution of the compounds formed by the interfacial reaction, mapping analysis was performed via energy-dispersive X-ray spectroscopy (EDS, Ultim-Max 170, Oxford, UK) combined with FE-SEM.

2.3. XRD

X-ray diffraction (XRD) analysis was performed using a diffractometer equipped with a Cu target (D8 ADVANCE, Bruker, Germany). The measurements were conducted under conditions of 40 kV and 40 mA, with scans carried out over a 2θ range of 10°~80° at a step size of 0.01° and a scanning speed of approximately 4°/min. The samples were measured in bulk form.

2.4. Vickers hardness

The microhardness of the Ni crucibles was measured using a micro-Vickers hardness tester (MVK-E, Akashi, Japan). The measurements were conducted under a load of 100 gf (0.98 N) with a dwell time of 10 seconds. For each sample, at least five indentations were made on the polished cross-sectional surface, and the average value was taken to ensure reproducibility. All measurements were performed at room temperature under ambient conditions.

3. Results and Discussion

Figure 2 presents the EDS mapping analysis results of

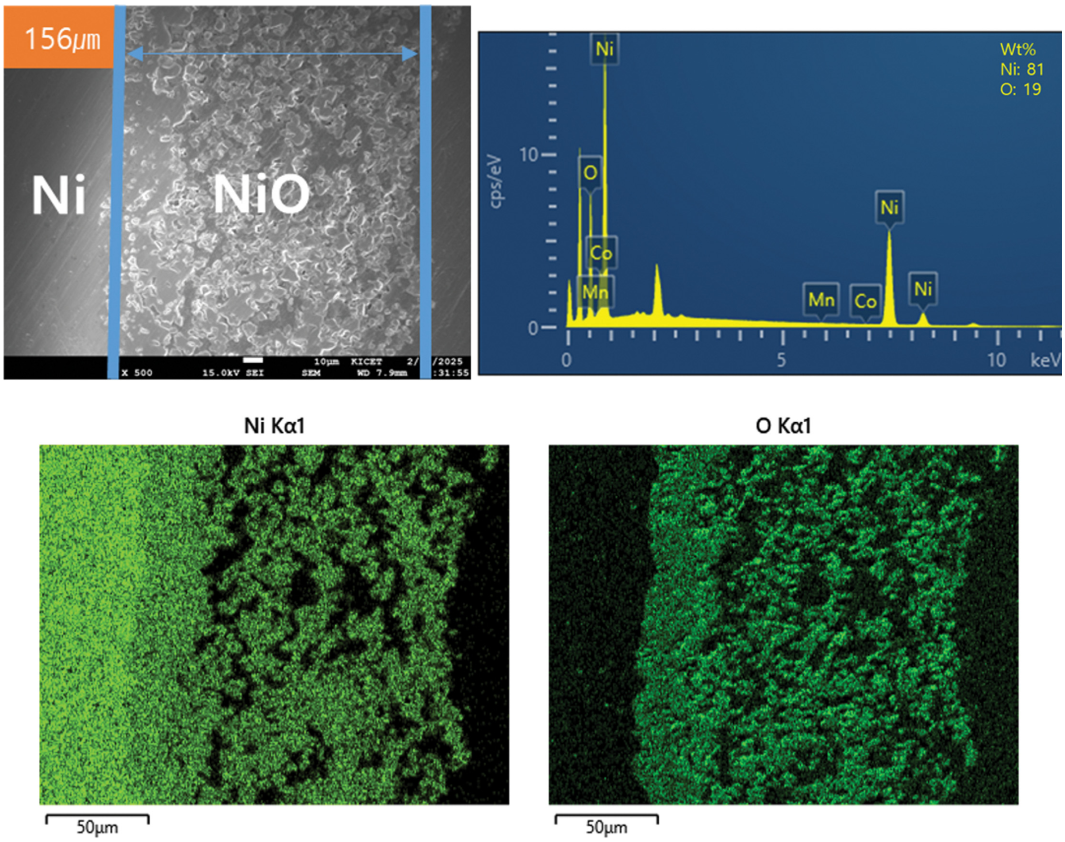

Fig. 2. FE-SEM-EDS images of the damaged saggar after heat treatment for 480 h at 900°C.

the internal surface reaction layer of the Ni metallic crucible heat-treated at 900°C for 480 h. The new phase formed on the surface was identified as nickel oxide. Additionally, a clear difference in oxygen concentration was observed between the surface reaction layer and the internal crucible layer of the Ni metallic crucible, while the oxygen concentration gradient in the surface reaction layer was not distinct. These results exhibited a similar trend to the observations in Study I [16].

Figure 3 shows the XRD patterns of the pristine Ni crucible and the Ni crucible heat-treated with NCM811 at 900°C for 480 h. While the pristine Ni crucible exhibited distinct diffraction peaks corresponding to metallic Ni, those peaks disappeared after heat treatment, and only peaks associated with NiO were observed. This result is consistent with the formation of NiO as confirmed by EDS analysis.

Figure 4 and 5 show the Vickers hardness indentations and hardness (HV) measurements of Ni crucibles in their original state and Ni crucibles heat-treated at 900°C for different periods of time, respectively. The specimen in Fig. 4(e) was difficult to measure due to the coarse grain structure formed on the surface.

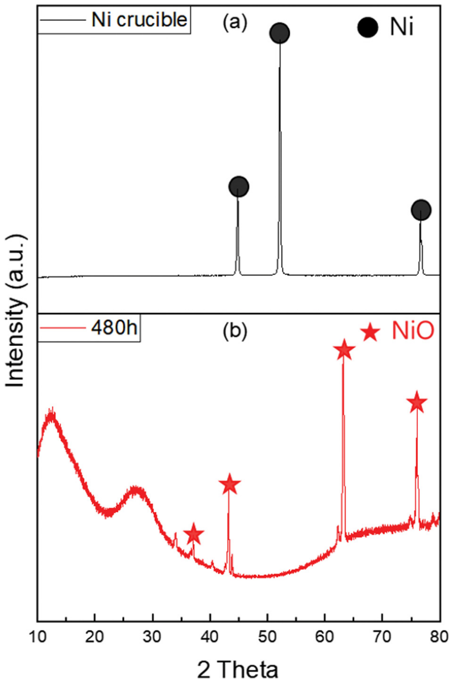

Fig. 3. XRD Patterns of (a) pristine Ni Crucible and (b) Ni Crucible Heat-Treated with NCM811 at 900°C for 480 h.

The Vickers hardness of the crucible heat-treated for 24 hours increased by approximately 3.5 times compared to the pure Ni crucible before heat treatment,

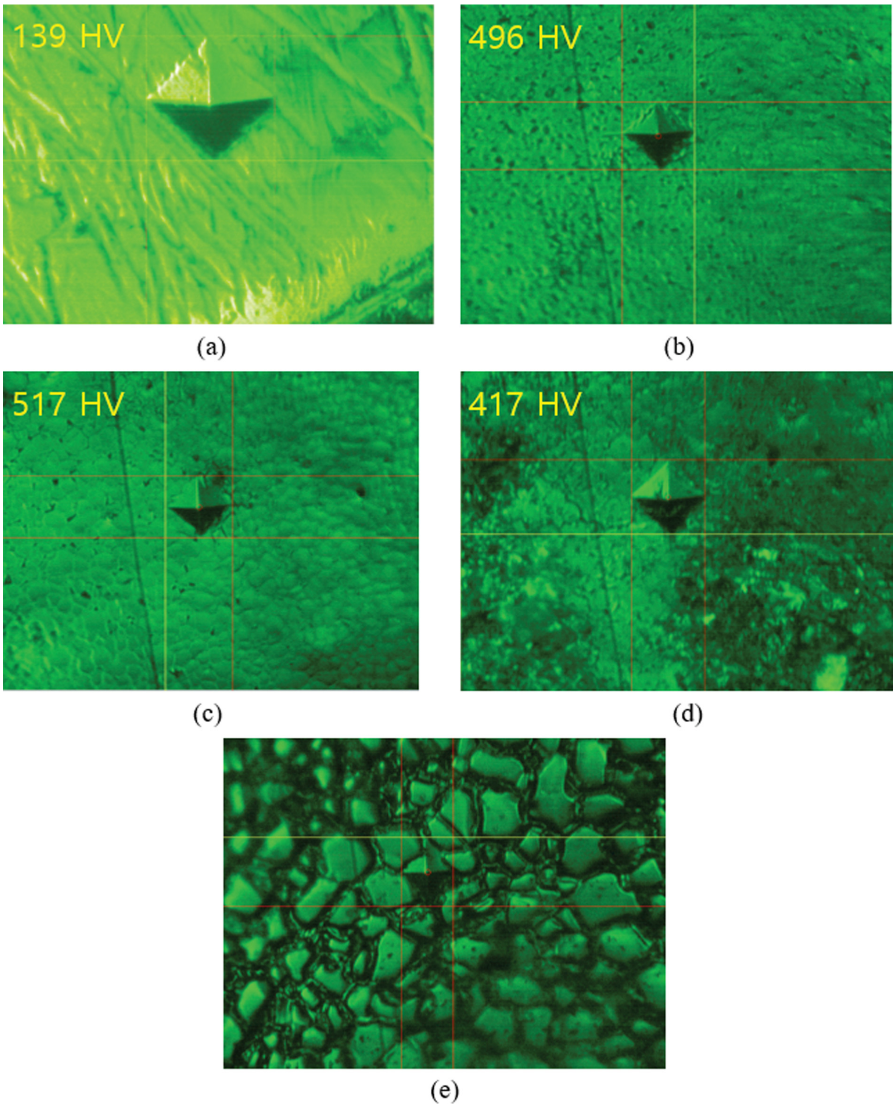

(a) (b) (c) (d) (e)

Fig. 4. Optical microscope images of Vickers indentations on Ni crucibles: (a) pristine Ni crucible, and Ni crucibles reacted with NCM811 at 900°C for (b) 24 h, (c) 48 h, (d) 72 h, and (e) 480 h.

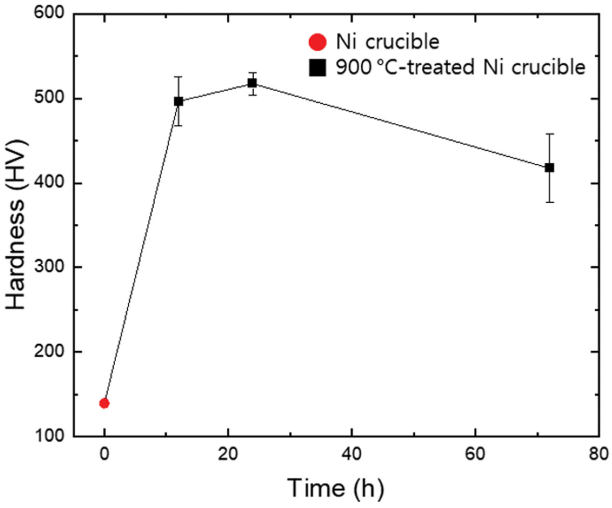

Fig. 5. Vickers hardness (H_v) of pristine Ni crucible and Ni crucibles heat-treated with NCM811 at 900°C for various durations.

which is judged to be due to the NiO oxide layer formed on the surface greatly improving the hardness. This is similar to the findings reported by Fasaki et al. in their study on NiO thin films, where an increase in substrate temperature led to larger grain sizes and reduced surface roughness, resulting in a tendency for hardness (approximately 418~989 HV) and elastic modulus (101~161 GPa) to increase [17].

On the other hand, although the hardness decreased slightly when the heat treatment time exceeded 48 hours, it still maintained a higher level than that of pure Ni crucibles. Therefore, although Ni crucibles exhibit increased brittleness after prolonged and repeated use at high temperatures, they still show potential for stable reuse in such conditions.

To analyze the reactivity based on the contact between the Ni metallic crucible and the anode precursor oxide, specimens were collected from the same position, as shown in Fig. 1. Figure 6 presents the changes in the thickness of the surface reaction layer depending on whether there was contact with the anode precursor oxide after 480 h of heat treatment. As shown in Fig. 6, even in specimens that did not come into contact with the anode precursor oxide, the thickness of the reaction layer tended to increase over time. This suggests that the reaction layer on the surface of the Ni metallic cru-

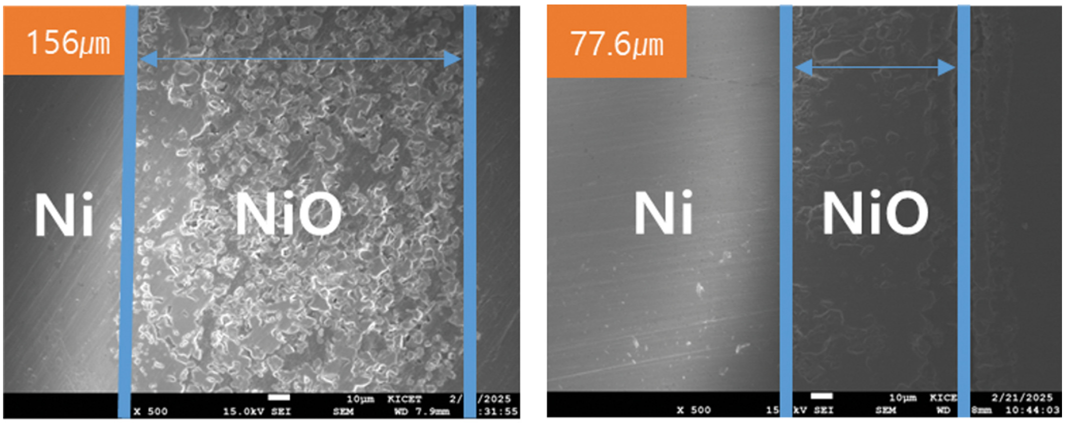

(a) (b)

Fig. 6. Cross-sectional microstructure images of nickel crucible at (a) 480 h with NCM 811, (b) 480 h without NCM 811 [16].

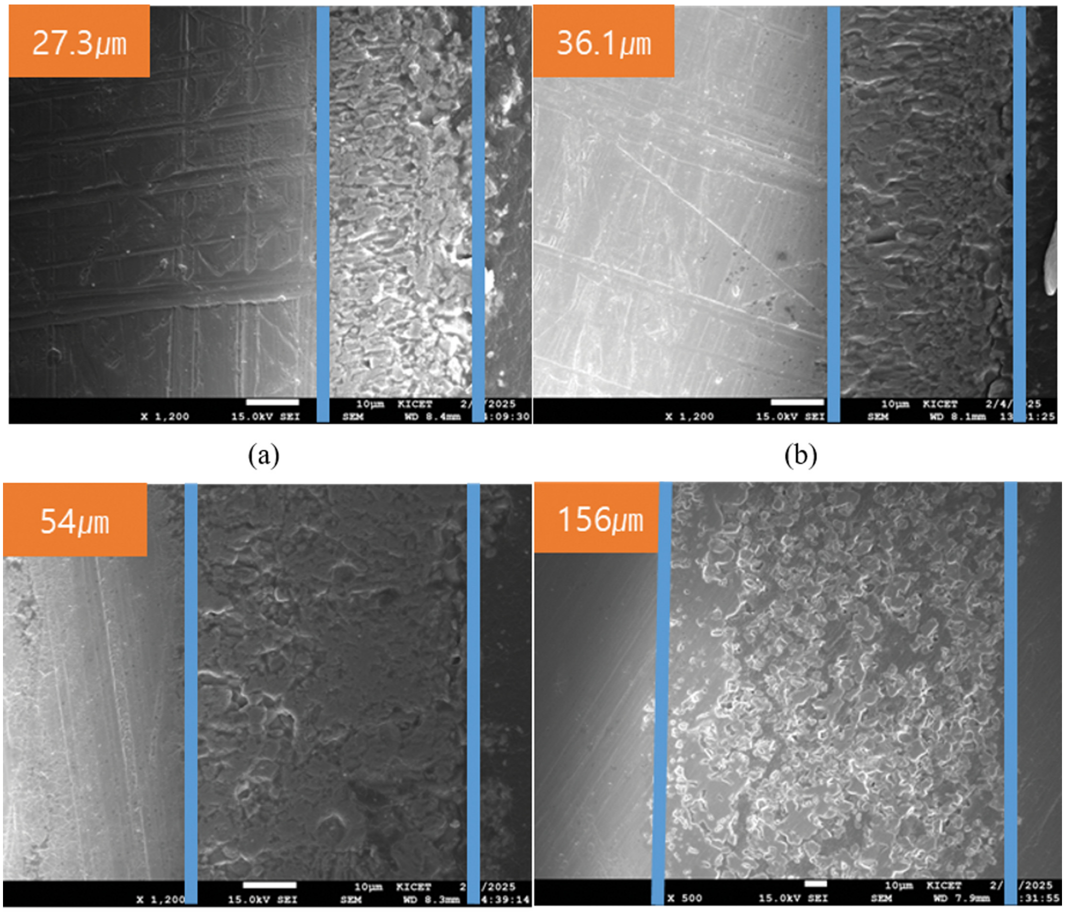

(a) (b)

(c) (d)

Fig. 7. Cross-sectional microstructure images of the nickel crucible reaction layer with retention times of (a) 12 h, (b) 24 h, (c) 72 h, and (d) 480 h. The magnification for images (a)~(c) is ×1200, and for image (d) is ×500.

Table 2
Comparison of the depth of the nickel crucible reaction layer according to retention time [16]

Time (h)	Reaction layer @bottom (µm)	
	$Ni_{0.8}Co_{0.1}Mn_{0.1}(OH)_2$ (Study I)	$LiNi_{0.8}Co_{0.1}Mn_{0.1}O_2$ (Study II)
12	9.0	27.3
24	15.0	36.1
72	27.0	54.0
480	99.0	156.0

cible was formed not only by oxygen diffused from the anode precursor oxide but also by oxygen from the high-temperature atmosphere. The thickness of the reaction layer on the specimen in contact with the anode precursor oxide was measured to be approximately 1.57 times greater than that of the specimen not in contact.

Figure 7 presents the changes in the surface reaction layer of the Ni crucible, as observed using FE-SEM, after heat treatment at 900°C for 12 to 480 h. Observation of the surface reaction layer revealed a dual microstructure in the oxide layer formed through reaction with the oxygen-rich cathode precursor material. This structure consists of a rough and irregular outer region and a relatively fine and porous inner region.

According to Unutulmazsoy and Haugsrud, when Ni is oxidized at 700°C, fine particle forms of oxide are formed at the oxide-metal and the oxide-gas interfaces, while the intermediate layer takes on a coarser columnar form. Additionally, when the oxidation temperature increases to 900°C, the rough pillar-shaped particles in the intermediate layer grow, forming a dual microstructure with a rough exterior and a fine porous interior [18,19].

Table 2 and Fig. 8 compare the depth of the reaction layer formed by $Ni_{0.80}Co_{0.10}Mn_{0.10}(OH)_2$ and $LiNi_{0.8}Co_{0.1}Mn_{0.1}O_2$ (with added Li), as observed in Study I, when they reacted with the Ni crucible. The results indicate that the reaction layer depth of $LiNi_{0.8}Co_{0.1}Mn_{0.1}O_2$ was approximately 1.6 to 3 times greater than that of $Ni_{0.80}Co_{0.10}Mn_{0.10}(OH)_2$. This suggests that the synthesis reaction of NCM with the Ni crucible proceeds more rapidly when Li is added. Both cases had an R-sq(mod) value exceeding 99 %, indicating reliable regression analysis results. In other words, during the NCM synthesis process, Li may have acted as a catalyst in the reaction with Ni, accelerating the growth of the reaction layer.

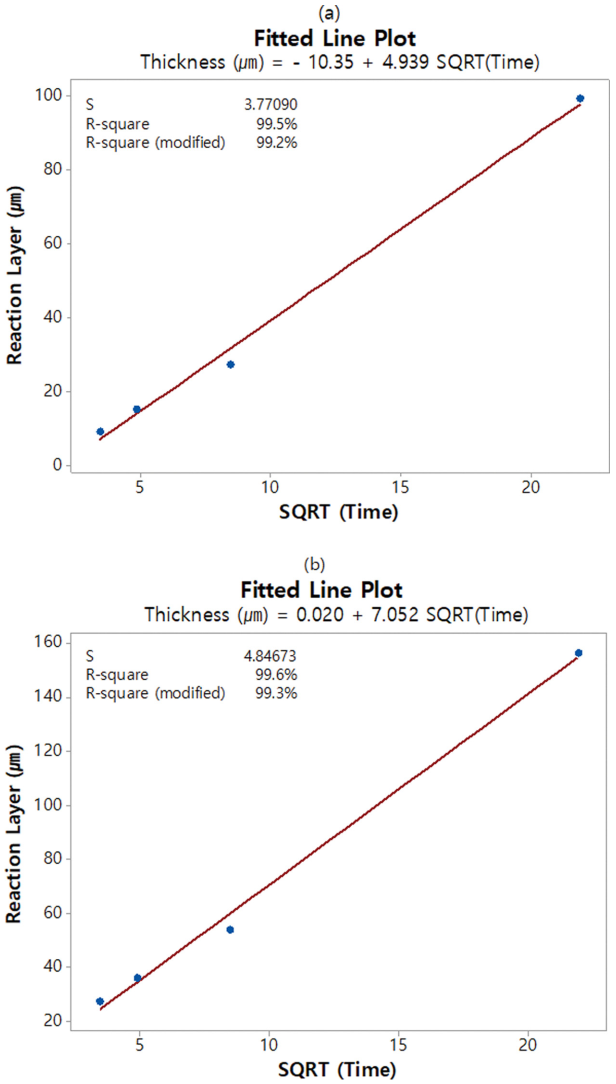

(a)
Fitted Line Plot
Thickness (µm) = - 10.35 + 4.939 SQRT(Time)

(b)
Fitted Line Plot
Thickness (µm) = 0.020 + 7.052 SQRT(Time)

Fig. 8. Comparison of the depth of the nickel crucible reaction layer for studies I and II according to the retention time [16].

According to the linear regression analysis presented in Fig. 8, the reaction layer formation rate (slope) was higher in the Li-containing sample (Study II) compared to the Li-free sample (Study I). Upon differentiation, Study I yields $f'(t) = (\frac{4.939}{2})\ t^{-1/2}$, and Study II yields $f'(t) = (\frac{7.052}{2})\ t^{-1/2}$. As $t \rightarrow \infty$, the slope approaches zero. This suggests that the growth rate of the reaction layer gradually decreases over time and may ultimately approach a saturation state.

This behavior is consistent with the parabolic rate law

Table 3
Variation of penetration constant of NiO_x with time [16]

Time (h)	Penetration constant (μm²/h)	
	$Ni_{0.8}Co_{0.1}Mn_{0.1}(OH)_2$ (Study I)	$LiNi_{0.8}Co_{0.1}Mn_{0.1}O_2$ (Study II)
12	6.75	62.11
24	9.38	54.30
72	10.13	40.50
480	20.42	50.70

$X^2 = K_p \cdot t$, which applies when the oxidation process is diffusion-controlled. According to this law, the oxide layer thickness X increases in proportion to the square root of time t. Differentiating with respect to time yields the instantaneous growth rate as $(dX/dt) = (K_p/2X)$. This indicates that as the oxide layer becomes thicker, the diffusion distance increases, and consequently, the growth rate gradually decreases [18].

Based on these results, the experimentally derived regression equation can be used to estimate the expected service life of the crucible. If the reaction layer reaches thicknesses of 200 μm, 400 μm, and 780 μm, the corresponding usable durations are predicted to be approximately 33.5 days, 134.0 days, and 509.7 days, respectively.

Cho et al. measured the thickness of the metal thin film and applied the formula [(reaction layer thickness)²/reaction time] to obtain the penetration constant [20].

In this study, as shown in Table 3, the NiO_x penetration constants of the $LiNi_{0.8}Co_{0.1}Mn_{0.1}O_2$ and $Ni_{0.8}Co_{0.1}Mn_{0.1}(OH)_2$ precursors were compared based on their reaction with the Ni crucible. The penetration constant of $LiNi_{0.8}Co_{0.1}Mn_{0.1}O_2$ was found to be approximately 2.5~9.2 times higher than that of $Ni_{0.8}Co_{0.1}Mn_{0.1}(OH)_2$. This is because $LiNi_{0.8}Co_{0.1}Mn_{0.1}O_2$ is known to generate highly permeable Li_2O during the sintering process, forming compounds containing Li_2O and inducing cracking [8]. However, as Li cannot be detected using the EDS analysis employed in this study, further research is needed to understand the diffusion-related mechanisms.

According to the findings thus far, conventional cordierite-based saggar is limited to approximately 10 uses and contributes to environmental pollution upon disposal. In contrast, the Ni crucible has been confirmed to be reusable for more than 480 h (approximately 20 d), demonstrating its high potential as a saggar material. Additionally, Ni crucibles used for extended periods can be recycled through reduction smelting, making them advantageous from an environmental perspective. Considering these characteristics, the Ni crucible is expected to be an effective alternative that meets the requirements for long-term durability and environmental sustainability in the NCM synthesis process.

As a follow-up study, a comparative analysis will be conducted between Ni crucibles and ceramic crucibles over time using NCM [$Li(Ni_xCo_yMn_z)O_2$] cathode active materials. The composition of the precursors synthesized in each type of crucible will be compared, and batteries will be fabricated to evaluate the differences in their performance.

4. Conclusions

In this study, a nickel metallic crucible and $LiNi_{0.8}Co_{0.1}Mn_{0.1}O_2$ (NCM 811) precursor were reacted for an extended period, and the changes in the crucible surface reaction layer over time were analyzed. As a result of the heat treatment at 900°C for 12 h to 480 h, the NiO_x/Ni diffusion interface structure exhibited continuous growth over time, and the formation of NiO_x was confirmed through FE-SEM-EDS analysis. Additionally, the analysis of the internal oxide content of Ni confirmed that the diffusion reaction at the interface progressively increased.

For Li-doped NCM 811, the thickness of the surface reaction layer increased by approximately 2~3 times compared to Study I. Additionally, the infiltration rate was found to be 2.5~9.2 times higher. Moreover, the surface hardness increased as a result of NiO layer formation. Nevertheless, after 480 h of heat treatment, the depth of the reaction layer remained only about one-fifth of the thickness of the Ni crucible. Based on these results, the Ni metal saggar can be used for more than 480 hours (20 days) in the synthesis process of NCM cathode active materials, confirming that it is a material with long-term durability.

Acknowledgement

This study was funded by the Ministry of Trade, Industry and Energy's Materials and Components Technology Development Project (Project Name: Development of Manufacturing Technology for Lithium High Corrosion-Resistant Refractory Ceramic Parts for High-Ni Secondary Battery Cathodes, Project Number 20024235, Project Unique Number. 1415187563).

References

[1] M. Winter and R.J. Brodd, "What are batteries, fuel cells, and supercapacitors?", Chem. Rev. 104 (2004) 4245.

[2] J. Yan, H. Huang, J. Tong, W. Li, X. Liu, H. Zhang, H. Huang and W. Zhou, "Recent progress on the modification of high nickel content NCM: Coating, doping, and single crystallization", Interdiscip. Mater. 1 (2022) 12043.

[3] F. Cerdas, P. Titscher, N. Bognar, R. Schmuch, M. Winter, A. Kwade and C. Herrmann, "Exploring the effect of increased energy density on the environmental impacts of traction batteries: A comparison of energy optimized lithium-ion and lithium-sulfur batteries for mobility applications", Energies 11 (2018) 150.

[4] G.E. Blomgren, "The development and future of lithium ion batteries", J. Electrochem. Soc. 164 (2017) A5019.

[5] Y. Wang, B. Liu, Q. Li, S. Cartmell, S. Ferrara, Z.D. Deng and J. Xiao, "Lithium and lithium ion batteries for applications in microelectronic devices: A review", J. Power Sources 286 (2015) 330.

[6] L. Britala, M. Marinaro and G. Kucinskis, "A review of the degradation mechanisms of NCM cathodes and corresponding mitigation strategies", J. Energy Storage 73 (2023) 108875.

[7] NMCA – a new high-performance cathode for Lithium-ion batteries used in EVs, EVreporter, https://evreporter.com/nmca-cathode-for-lithium-ion-batteries/, 2021.

[8] M. Ju, Y. Liang, S. Li, M. Cai, J. Nie and Z. Shan, "Superior corrosion resistance spinel-containing sagger material for calcining Li-ion battery cathode material", J. Ceram. Soc. Jpn. 128 (2020) 368.

[9] H.J. Kim, H.T. Kim and S.S. Ryu, "Sagger for synthesizing positive electrode active material of secondary battery and manufacturing method of the same", Korea Patent Application No. 1020120038227, Application Date 20120413, Registration Date 20131023.

[10] U.S. Kim, J.H. Kim, K.S. Han, J.H. Choi and K.T. Hwang, "Sagger for synthesizing cathode active material of secondary battery, its manufacturing method, and glaze for it", Korea Patent Application No. 1020230101393, Application Date 20230803.

[11] J.H. Kim, D.S. Kim, S.U. Choi and J.H. Kim, "Sagger for synthesizing electrode active material of secondary battery", Korea Patent Application No. 1020180125034, Application Date 20181019, Registration Date 20200113.

[12] J.H. Kim and I.K. Hwang, "Co-precipitation reactor for composing a big concentrat gradient precurs and this method", Korea Patent Application No. 1020160171847, Application Date 20161215, Registration Date 20181112.

[13] K.P. Hong and S.S. Kim, "Reuse method of sagger for manufacturing positive electrode active material and sagger using same", Korea Patent Application No. 1020210181050, Application Date 20211216.

[14] J.L. White, F.S. Gittleson, M. Homer and F. El Gabaly, "Nickel and cobalt oxidation state evolution at Ni-rich NMC cathode surfaces during treatment", J. Phys. Chem. C 124 (2020) 16508.

[15] W.L. Phillips Jr., "Oxidation rates of pure and less pure nickel", J. Electrochem. Soc. 110 (1963) 1015.

[16] Y.I. Park, J.H. Jung, S.H. Woo, J.H. Lee and H.J. Kim, "Study on the feasibility of metallic saggar for synthesizing NCM cathode active materials-I", J. Korean Cryst. Growth Cryst. Technol. 34 (2024) 103.

[17] I. Fasaki, A. Koutoulaki, M. Kompitsas and C. Charitidis, "Structural, electrical and mechanical properties of NiO thin films grown by pulsed laser deposition", Appl. Surf. Sci. 257 (2010) 429.

[18] Y. Unutulmazsoy, R. Merkle, D. Fischer, J. Mannhart and J. Maier, "The oxidation kinetics of thin nickel films between 250 and 500°C", Phys. Chem. Chem. Phys. 19 (2017) 9045.

[19] R. Haugsrud, "On the high-temperature oxidation of nickel", Corrosion Science 45 (2003) 211.

[20] J.S. Cho and D.H. KIm, "Formation of TiNi intermetallics by a diffusion reaction at Ti/Ni multi-layer interface", J. of the Korean Inst. of Met. & Mater. 35 (1997) 1439.